

Metal–Metal Bonding in Binuclear Metal Carbonyls with Three Bridging Methylaminobis(difluorophosphine) Ligands: Iron, Cobalt, and Nickel Derivatives

Rong Zou,[†] Qian-shu Li,^{*,†,‡} Yaoming Xie,[§] R. Bruce King,^{*,†,§} and Henry F. Schaefer III[§]

[†]Center for Computational Quantum Chemistry, South China Normal University, Guangzhou 510631, P.R. China, [‡]Institute of Chemical Physics, Beijing Institute of Technology, Beijing 100081, P.R. China, and [§]Department of Chemistry and Center for Computational Chemistry, University of Georgia, Athens, Georgia 30602

Received October 27, 2009

The $[\text{CH}_3\text{N}(\text{PF}_2)_2]_3\text{M}_2(\text{CO})_n$ ($\text{M} = \text{Fe}, \text{Co}, \text{Ni}; n = 2, 1, 0$) derivatives, in which a metal–metal bond is bridged by three $\text{CH}_3\text{N}(\text{PF}_2)_2$ groups similar to the known very stable $[\text{CH}_3\text{N}(\text{PF}_2)_2]_3\text{Co}_2(\text{CO})_2$, have been investigated by density functional theory. The lowest energy structures for the dicarbonyls $[\text{CH}_3\text{N}(\text{PF}_2)_2]_3\text{M}_2(\text{CO})_2$ ($\text{M} = \text{Ni}, \text{Co}, \text{Fe}$) are predicted to be closed-shell singlets with metal–metal distances of ~ 3.94 Å, ~ 2.80 Å, and ~ 2.63 Å, respectively, corresponding to the metal–metal bonds of orders 0, 1, and 2, required to give both metal atoms the favored 18-electron configurations. For the monocarbonyls $[\text{CH}_3\text{N}(\text{PF}_2)_2]_3\text{M}_2(\text{CO})$ ($\text{M} = \text{Ni}, \text{Co}, \text{Fe}$), unsymmetrical structures with a carbonyl group terminally bonded to one metal are greatly preferred energetically over structures in which the carbonyl group bridges the pair of metal atoms. The lowest energy structures for $[\text{CH}_3\text{N}(\text{PF}_2)_2]_3\text{M}_2(\text{CO})$ ($\text{M} = \text{Ni}, \text{Co}, \text{Fe}$) are singlet, triplet, and singlet states, respectively, with metal–metal distances of ~ 2.77 Å, ~ 2.38 Å, and ~ 2.13 Å, respectively. These distances correspond to the metal–metal dative bonds of orders 1, 2, and 3, required to give both metal atoms the favored 18-electron configuration. Among the carbonyl-free species the iron compound $[\text{CH}_3\text{N}(\text{PF}_2)_2]_3\text{Fe}_2$ is of particular interest since its very short $\text{Fe}\equiv\text{Fe}$ distance of ~ 2.02 Å suggests the formal quadruple bond required to give both iron atoms the favored 18-electron configuration.

1. Introduction

A major area of coordination chemistry is the chemistry of transition metals in low, zero, and even negative formal oxidation states incorporating strong π -acceptor (“back bonding”) ligands. The classical ligand of this type is carbon monoxide, leading, for example, to the stable zerovalent metal carbonyls¹ $\text{Ni}(\text{CO})_4$, $\text{Fe}(\text{CO})_5$, and $\text{Cr}(\text{CO})_6$. More recently, phosphorus trifluoride (trifluorophosphine) has been shown to form even more stable analogous zerovalent metal complexes.^{2,3} The synthesis of extensive series of metal carbonyl and trifluorophosphine derivatives is facilitated by the ready availability in quantity of the free ligands, namely, carbon monoxide and phosphorus trifluoride. Thus both CO and PF_3 are stable gases that can be used even in high pressure reactions with suitable transition metal derivatives.

Both CO and PF_3 are, of course, monodentate ligands. Chelating ligands incorporating similar donor/acceptor functionalities are of interest since they should form even more stable low oxidation state transition metal derivatives than

CO and PF_3 . However, the design and synthesis of such ligands have posed some major challenges because of the chelate effect. Thus carbon monoxide clearly has no “handle” for incorporation into a polydentate ligand structure. Bidentate and polydentate ligands related to PF_3 containing two or more PF_2 donor groups are more promising possibilities.

The most readily available ligands containing two PF_2 donor groups in suitable positions to form chelate rings are the alkylaminobis(difluorophosphines) $\text{RN}(\text{PF}_2)_2$. The methyl derivative ($\text{R} = \text{CH}_3$) is accessible as a volatile, readily handled stable liquid, in quantities of 100 g or larger through a simple two-step synthesis with the relatively inexpensive methylammonium chloride, phosphorus trichloride, and antimony trifluoride as raw materials.⁴ The first transition metal complexes of the $\text{CH}_3\text{N}(\text{PF}_2)_2$ ligand were synthesized by Nixon and co-workers.^{5,6} Subsequently, the low oxidation state transition metal chemistry of $\text{CH}_3\text{N}(\text{PF}_2)_2$ was developed extensively by one of the authors (R.B.K.) approximately 30 years ago at the University of Georgia.⁷

*To whom correspondence should be addressed. E-mail: rbking@chem.uga.edu.

(1) Cotton, F. A. *Prog. Inorg. Chem.* **1976**, 21, 1.
(2) Kruck, T. *Angew. Chem., Int. Ed. Engl.* **1967**, 6, 53.
(3) Nixon, J. F. *Adv. Inorg. Chem. Radiochem.* **1985**, 29, 41.

(4) Nixon, J. F. *J. Chem. Soc. A* **1968**, 2689.
(5) Johnson, T. R.; Nixon, J. F. *J. Chem. Soc. (A)* **1969**, 2518.
(6) Nixon, J. F.; Pinkerton, A. A. *J. Organomet. Chem.* **1972**, 37, C47.
(7) King, R. B. *Acc. Chem. Res.* **1980**, 13, 243.

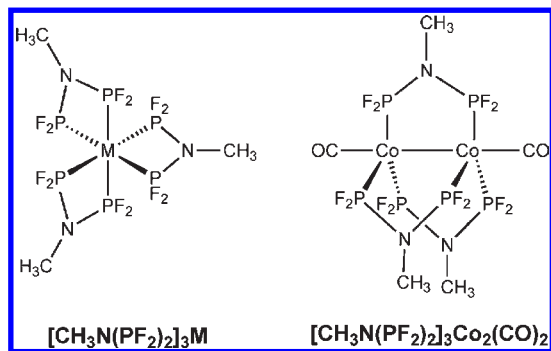


Figure 1. Structures of $[\text{CH}_3\text{N}(\text{PF}_2)_2]_3\text{M}$ ($\text{M} = \text{Cr}, \text{Mo}, \text{W}$) and $[\text{CH}_3\text{N}(\text{PF}_2)_2]_3\text{Co}_2(\text{CO})_2$.

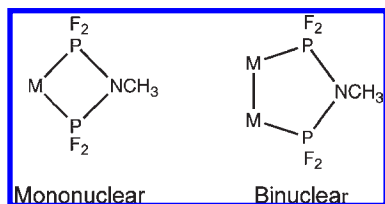


Figure 2. Chelate rings formed by $\text{CH}_3\text{N}(\text{PF}_2)_2$ in mononuclear and binuclear metal complexes.

The anticipated ability of $\text{CH}_3\text{N}(\text{PF}_2)_2$ to stabilize low oxidation state transition metal derivatives was realized in the variety of its complexes that were synthesized at that time.⁷ Thus photolysis of the metal hexacarbonyls $\text{M}(\text{CO})_6$ ($\text{M} = \text{Cr}, \text{Mo}, \text{W}$) with excess $\text{CH}_3\text{N}(\text{PF}_2)_2$ resulted in complete displacement of all six carbonyl groups to give the zerovalent complexes $[\text{CH}_3\text{N}(\text{PF}_2)_2]_3\text{M}$ ($\text{M} = \text{Cr}, \text{Mo}, \text{W}$) as white volatile solids (Figure 1).^{8,9} The stability of these zerovalent metal complexes is dramatic. Thus $[\text{CH}_3\text{N}(\text{PF}_2)_2]_3\text{Cr}$ melts at 182–183 °C, and then, at least in a melting point capillary, the resulting yellow liquid at atmospheric pressure boils at ~256 °C.

The mononuclear $\text{CH}_3\text{N}(\text{PF}_2)_2$ chelates such as $[\text{CH}_3\text{N}(\text{PF}_2)_2]_3\text{Cr}$ are interesting since the MP_2N chelate rings are carbon-free and contain only four atoms (Figure 2) rather than the five or six atoms typical for chelate rings. However, binuclear $\text{CH}_3\text{N}(\text{PF}_2)_2$ complexes are also possible containing five-membered $\text{M}_2\text{P}_2\text{N}$ rings (Figure 2). Such a complex of particular interest is the very stable purple cobalt carbonyl derivative $[\text{CH}_3\text{N}(\text{PF}_2)_2]_3\text{Co}_2(\text{CO})_2$, which is readily obtained in good yield by the reaction of $\text{Co}_2(\text{CO})_8$ with $\text{CH}_3\text{N}(\text{PF}_2)_2$ at room temperature.^{10,11} In the structure of $[\text{CH}_3\text{N}(\text{PF}_2)_2]_3\text{Co}_2(\text{CO})_2$ the cobalt–cobalt bond is bridged by three bidentate $\text{CH}_3\text{N}(\text{PF}_2)_2$ ligands leading to three five-membered $\text{Co}_2\text{P}_2\text{N}$ chelate rings sharing the Co–Co bond (Figure 1). The resulting $[\text{CH}_3\text{N}(\text{PF}_2)_2]_3\text{Co}_2$ unit is so stable that it remains intact when $[\text{CH}_3\text{N}(\text{PF}_2)_2]_3\text{Co}_2$ unit is brominated¹² to give $[\text{CH}_3\text{N}(\text{PF}_2)_2]_3\text{Co}_2\text{Br}_4$ or reduced to the radical anion¹³ $\{[\text{CH}_3\text{N}(\text{PF}_2)_2]_3\text{Co}_2(\text{CO})_2\}^\bullet$. In addition, this unit remains intact upon photolysis and is the basis of an

interesting photocatalytic olefin isomerization system.¹⁴ Furthermore, the two linked rhodium(II) sites in the related binuclear triply bridged rhodium(II) bromide derivative $[\text{CH}_3\text{N}(\text{PF}_2)_2]_3\text{Rh}_2\text{Br}_4$ provide the basis for novel four-electron photochemistry based on the reduction of the rhodium(II) sites to rhodium(0) sites.¹⁵

These observations on $[\text{CH}_3\text{N}(\text{PF}_2)_2]_3\text{Co}_2(\text{CO})_2$ suggest that the potential chemistry of triply bridged $[\text{CH}_3\text{N}(\text{PF}_2)_2]_3\text{M}_2$ units as inseparable entities can be rather extensive. To assess the possibilities in this area, we have used density functional theory to study the first row transition metal carbonyl derivatives $[\text{CH}_3\text{N}(\text{PF}_2)_2]_3\text{M}_2(\text{CO})_n$ ($n = 2, 1, 0$). Our results in this area are presented in this paper.

2. Theoretical Methods

Electron correlation effects were considered using density functional theory (DFT) methods, which have evolved as a practical and effective computational tool, especially for organometallic compounds.^{16–30} Thus two DFT methods were used in this study. The first functional is the B3LYP method, which is the hybrid HF/DFT method using a combination of the three-parameter Becke functional (B3) with the Lee–Yang–Parr (LYP) generalized gradient correlation functional.^{31,32} The other DFT method used in the present paper is BP86, which combines Becke's 1988 exchange functional (B) with Perdew's 1986 gradient corrected correlation functional method (P86).^{33,34}

All computations were performed using double- ζ plus polarization (DZP) basis sets. For the C, N, O, and F atoms, the double- ζ plus polarization (DZP) basis sets are the Huzinaga–Dunning contracted double- ζ sets^{35,36} plus a set of spherical harmonic d polarization functions with orbital exponents $\alpha_d(\text{C}) = 0.75$, $\alpha_d(\text{N}) = 0.80$, $\alpha_d(\text{O}) = 0.85$, and $\alpha_d(\text{F}) = 1.0$, and, designated as (9s5p1d/4s2p1d). The DZP basis sets used for phosphorus add a set of polarization d functions with $\alpha_d(\text{P}) = 0.6$ to Dunning's DZ (11s7p1d/6s4p1d) set.³⁷ For hydrogen, a set of p polarization functions $\alpha_p(\text{H}) = 0.75$ is added to the Huzinaga–Dunning DZ set.

(14) Richmond, M. G.; Pittman, C. U., Jr. *J. Mol. Catal.* **1989**, *53*, 79.

(15) Heyduk, A. F.; Macintosh, A. M.; Nocera, D. G. *J. Am. Chem. Soc.* **1999**, *121*, 5023.

(16) Ehlens, A. W.; Frenking, G. *J. Am. Chem. Soc.* **1994**, *116*, 1514.

(17) Delley, B.; Wrinn, M.; Lüthi, H. P. *J. Chem. Phys.* **1994**, *100*, 5785.

(18) Li, J.; Schreckenbach, G.; Ziegler, T. *J. Am. Chem. Soc.* **1995**, *117*, 486.

(19) Jonas, V.; Thiel, W. *J. Phys. Chem.* **1995**, *102*, 8474.

(20) Barckholtz, T. A.; Bursten, B. E. *J. Am. Chem. Soc.* **1998**, *120*, 1926.

(21) Niu, S.; Hall, M. B. *Chem. Rev.* **2000**, *100*, 353.

(22) Macchi, P.; Sironi, A. *Coord. Chem. Rev.* **2003**, *238*, 383.

(23) Buhl, M.; Kabrede, H. *J. Chem. Theory Comput.* **2006**, *2*, 1282.

(24) Tonner, R.; Heydenrych, G.; Frenking, G. *J. Am. Chem. Soc.* **2008**, *130*, 8952.

(25) Ziegler, T.; Autschbach, J. *Chem. Rev.* **2005**, *105*, 2695.

(26) Waller, M. P.; Bühl, M.; Geethanakshmi, K. R.; Wang, D.; Thiel, W. *Chem.—Eur. J.* **2007**, *13*, 4723.

(27) Hayes, P. G.; Beddie, C.; Hall, M. B.; Waterman, R.; Tilley, T. D. *J. Am. Chem. Soc.* **2006**, *128*, 428.

(28) Bühl, M.; Reimann, C.; Pantazis, D. A.; Bredow, T.; Neese, F. *J. Chem. Theory Comput.* **2008**, *4*, 1449.

(29) Besora, M.; Carreon-Macedo, J.-L.; Cowan, J.; George, M. W.; Harvey, J. N.; Portius, P.; Ronayne, K. L.; Sun, X.-Z.; Towrie, M. *J. Am. Chem. Soc.* **2009**, *131*, 3583.

(30) Ye, S.; Tuttle, T.; Bill, E.; Simkhorich, L.; Gross, Z.; Thiel, W.; Neese, F. *Chem.—Eur. J.* **2008**, *14*, 10839.

(31) Becke, A. D. *J. Chem. Phys.* **1993**, *98*, 5648.

(32) Lee, C.; Yang, W.; Parr, R. G. *Phys. Rev. B* **1988**, *37*, 785.

(33) Becke, A. D. *Phys. Rev. A* **1988**, *38*, 3098.

(34) Perdew, J. P. *Phys. Rev. B* **1986**, *33*, 8822.

(35) Dunning, T. H. *J. Chem. Phys.* **1970**, *53*, 2823.

(36) Huzinaga, S. *J. Chem. Phys.* **1965**, *42*, 1293.

(37) Dunning, T. H.; Hay, P. In *Modern Theoretical Chemistry*; Schaefer, H. F., Ed.; Plenum Press: New York, 1977; Vol 3.

(8) King, R. B.; Gimeno, J. *Chem. Commun.* **1977**, 142.

(9) King, R. B.; Gimeno, J. *Inorg. Chem.* **1978**, *17*, 2390.

(10) Newton, M. G.; King, R. B.; Chang, M.; Pantaleo, N. S.; Gimeno, J. *Chem. Commun.* **1977**, 531.

(11) King, R. B.; Gimeno, J.; Lotz, T. J. *Inorg. Chem.* **1978**, *17*, 2401.

(12) Newton, M. G.; Pantaleo, N. S.; King, R. B.; Lotz, T. J. *Chem. Commun.* **1975**, 514.

(13) Chaloyard, A.; El Murr, N.; King, R. B. *J. Organomet. Chem.* **1980**, *188*, C13.

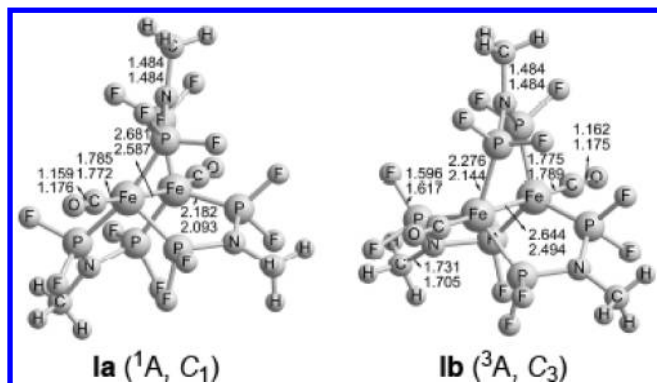


Figure 3. Two optimized $[\text{CH}_3\text{N}(\text{PF}_2)_2]_3\text{Fe}_2(\text{CO})_2$ structures.

The loosely contracted DZP basis set for the transition metal (Fe, Co, or Ni) is the Wachters primitive set³⁸ augmented by two sets of p functions and a set of d functions, contracted following Hood, Pitzer, and Schaefer,³⁹ and designated (14s11p6d/10s8p3d).

The geometries of all of the structures were fully optimized using the DZP B3LYP and DZP BP86 methods with the Gaussian 03 program.⁴⁰ The fine grid option (75 radial shells, 302 angular points) was used for numerical evaluation of the integrals. The tight (10^{-8} hartree) designation was the default for the self-consistent field (SCF) convergence.

The vibrational frequencies were determined by evaluating analytically the second derivatives of the energy with respect to the nuclear coordinates. The corresponding infrared intensities were also evaluated analytically. Low magnitude imaginary vibrational frequencies are suspect because of significant limitations in the numerical integration procedures used in the current DFT computations.⁴¹ Thus all imaginary vibrational frequencies with magnitudes less than $100i\text{ cm}^{-1}$ are considered questionable, and are given less weight in the analysis.^{41–43} Therefore, we do not always follow such low imaginary vibrational frequencies. In critical situations the computations were confirmed using finer numerical integration grids (120 radial shells, 974 angular points).

The insignificance of imaginary vibrational frequencies less than $100i\text{ cm}^{-1}$ was checked with the structures **IIc**, **Vb**, and **VIIIb**, all of which lie at relatively high energies (23 to 66 kcal/mol) above the corresponding global minima. The imaginary frequencies of these structures were found to correspond to methyl group rotation. Following the corresponding normal modes led to very little change in either the optimized structures (only $\sim 5^\circ$ rotation of the methyl groups) or the relative energies (< 0.01 kcal/mol).

3. Results

3.1. $[\text{CH}_3\text{N}(\text{PF}_2)_2]_3\text{Fe}_2(\text{CO})_2$. Two structures for $[\text{CH}_3\text{N}(\text{PF}_2)_2]_3\text{Fe}_2(\text{CO})_2$ were found (Figure 3 and Table 1). The global minimum is the singlet structure **Ia** without any imaginary frequencies. Each iron atom bears a single terminal carbonyl group. These carbonyl groups are predicted to exhibit a strong $\nu(\text{CO})$ frequency at 1971 cm^{-1} and a weak $\nu(\text{CO})$ frequency at 1981 cm^{-1} .

Table 1. Total Energies (E in kcal/mol), Relative Energies (ΔE in kcal/mol), Fe–Fe Distances (\AA), and Spin Expectation Values ($\langle S^2 \rangle$) for the Two Optimized structures $[\text{CH}_3\text{N}(\text{PF}_2)_2]_3\text{Fe}_2(\text{CO})_2$

	Ia (C_1)		Ib (C_3)	
	B3LYP	BP86	B3LYP	BP86
$-E$	6285.38501	6285.98337	6285.38229	6285.96822
ΔE	0.0	0.0	1.7	9.5
Fe–Fe	2.681	2.587	2.644	2.494
$\langle S^2 \rangle$	0	0	2.26	2.03
imaginary frequencies	none	none	none	62i, 62i

The Fe=Fe distance in **Ia** is predicted to be 2.681 \AA (B3LYP) or 2.587 \AA (BP86), which is consistent with the formal double bond required to give each iron atom the favored 18-electron configuration.

The triplet $[\text{CH}_3\text{N}(\text{PF}_2)_2]_3\text{Fe}_2(\text{CO})_2$ structure **Ib** lies energetically above **Ia** by 1.7 kcal/mol (B3LYP) or 9.5 kcal/mol (BP86) (Figure 3 and Table 1). However, the predicted relative energy of **Ib** using B3LYP may be lower than the real value because of serious spin contamination ($\langle S^2 \rangle = 2.26$). The Fe=Fe distance in the $[\text{CH}_3\text{N}(\text{PF}_2)_2]_3\text{Fe}_2(\text{CO})_2$ triplet **Ib** is predicted to be 2.644 \AA (B3LYP) or 2.494 \AA (BP86), which is shorter than that in **Ia** but still can correspond to the formal double bond needed to give both iron atoms the favored 18-electron configuration. In this case, the double bond in **Ib** may be of the $\sigma + ^2/2\pi$ type, similar to that found in triplet dioxygen or the organometallic compound^{44–46} $(\eta^5\text{-C}_5\text{H}_5)_2\text{Fe}_2(\mu\text{-CO})_3$ with single electrons in each of the two orthogonal π orbitals, thereby leading to the predicted triplet spin multiplicity.

3.2. $[\text{CH}_3\text{N}(\text{PF}_2)_2]_3\text{Fe}_2(\text{CO})$. Three structures are predicted for the monocarbonyl $[\text{CH}_3\text{N}(\text{PF}_2)_2]_3\text{Fe}_2(\text{CO})$ (Figure 4 and Table 2). The singlet structure **IIa** with C_1 symmetry and a terminal CO group is the global minimum of $[\text{CH}_3\text{N}(\text{PF}_2)_2]_3\text{Fe}_2(\text{CO})$, with all real harmonic vibrational frequencies. The terminal CO group is predicted to exhibit a $\nu(\text{CO})$ frequency at 1980 cm^{-1} . The $[\text{CH}_3\text{N}(\text{PF}_2)_2]_3\text{Fe}_2(\text{CO})$ structure **IIa** can be derived from the $[\text{CH}_3\text{N}(\text{PF}_2)_2]_3\text{Fe}_2(\text{CO})_2$ structure **Ia** by removing one of the terminal CO groups. The relatively short Fe=Fe distance in the $[\text{CH}_3\text{N}(\text{PF}_2)_2]_3\text{Fe}_2(\text{CO})$ structure **IIa** of 2.141 \AA (B3LYP) or 2.125 \AA (BP86) is reasonable for the formal polarized triple bond required to give both iron atoms the favored 18-electron configuration.

A C_3 symmetry triplet $[\text{CH}_3\text{N}(\text{PF}_2)_2]_3\text{Fe}_2(\text{CO})$ structure **IIb** is found to lie above **IIa** by 7.2 kcal/mol (B3LYP) or 36.6 kcal/mol (BP86) (Figure 4 and Table 2). The inconsistent relative energies predicted by the two methods can be explained by their different spin contaminations (Table 2). The Fe \cdots Fe distance of **IIb** is 3.164 \AA (B3LYP) or 2.993 \AA (BP86), suggesting only a weak interaction, at most, between the two Fe atoms. Spin density analysis by BP86 (chosen because of the lower spin contamination) suggests that both unpaired electrons are localized on the iron atom not bearing the carbonyl group. If the Fe \cdots Fe interaction is assumed

(38) Wachters, A. J. H. *J. Chem. Phys.* **1970**, *52*, 1033.

(39) Hood, D. M.; Pitzer, R. M.; Schaefer, H. F. *J. Chem. Phys.* **1979**, *71*, 705.

(40) Frisch, M. J. et al. *Gaussian 03*, Revision C 02; Gaussian, Inc: Wallingford, CT, 2004 (see Supporting Information for details).

(41) Papas, B. N.; Schaefer, H. F. *J. Mol. Struct.* **2006**, *768*, 175.

(42) Jacobsen, H.; Ziegler, T. *J. Am. Chem. Soc.* **1996**, *118*, 4631.

(43) Martin, J. M. L.; Bauschlicher, C. W.; Ricca, A. *Comput. Phys. Commun.* **2001**, *133*, 189.

(44) Caspar, J. V.; Meyer, T. J. *J. Am. Chem. Soc.* **1980**, *102*, 7794.

(45) Hooker, R. H.; Mahmoud, K. A.; Rest, A. *J. Chem. Commun.* **1983**, 1022.

(46) Hepp, A. F.; Blaha, J. P.; Lewis, C.; Wrighton, M. S. *Organometallics* **1984**, *3*, 174.

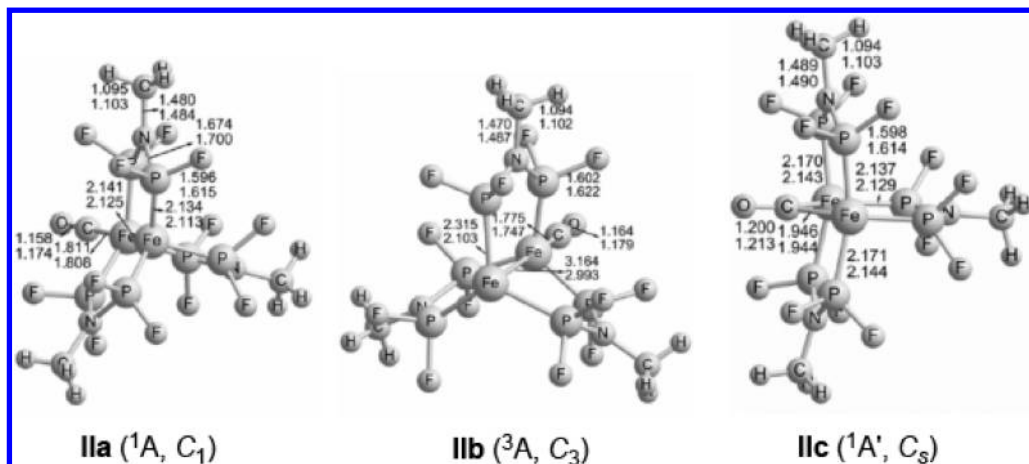


Figure 4. Three optimized $[\text{CH}_3\text{N}(\text{PF}_2)_2]_3\text{Fe}_2(\text{CO})$ structures.

Table 2. Total Energies (E in kcal/mol), Relative Energies (ΔE in kcal/mol), Fe–Fe distance (\AA), and Spin Expectation Values ($\langle S^2 \rangle$) for $[\text{CH}_3\text{N}(\text{PF}_2)_2]_3\text{Fe}_2(\text{CO})^a$

	IIa (C_1)		IIb (C_3)		IIc (C_s)	
	B3LYP	BP86	B3LYP	BP86	B3LYP	BP86
$-E$	6172.0092	6172.59226	6171.99775	6172.53402	6171.95594	6172.53088
ΔE	0.0	0.0	7.2	36.6	33.4	38.5
Fe–Fe	2.141	2.125	3.164	2.993	2.563	2.545
$\langle S^2 \rangle$	0	0	2.83	2.19	0	0
imaginary frequencies	none	none	none	none	70i,44i	74i,56i

^a Note that the two imaginary frequencies for **IIc** go away with a larger integration grid.

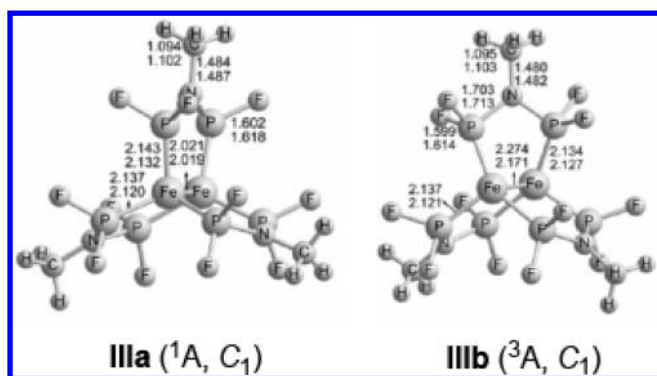


Figure 5. Two optimized $[\text{CH}_3\text{N}(\text{PF}_2)_2]_3\text{Fe}_2$ structures.

to be negligible, this iron atom in **IIb** has a 14-electron configuration, whereas the iron bearing the carbonyl group has a 16-electron configuration.

A second singlet $[\text{CH}_3\text{N}(\text{PF}_2)_2]_3\text{Fe}_2(\text{CO})$ structure **IIc** with a bridging CO group is predicted to lie at the rather high energy of 33.4 kcal/mol (B3LYP) or 38.5 kcal/mol (BP86) above the global minimum **IIa** (Figure 4 and Table 2). Structure **IIc** has two small imaginary vibrational frequencies, namely, 70i and 44i cm^{-1} (B3LYP) or 74i and 56i cm^{-1} (BP86). However, these two frequencies turn out to be real when a larger numerical integration grid (120 radial shells, 974 angular points) is used, suggesting that these imaginary frequencies arise from numerical integration errors.

3.3. $[\text{CH}_3\text{N}(\text{PF}_2)_2]_3\text{Fe}_2$. Two structures (one singlet and one triplet) were optimized for $[\text{CH}_3\text{N}(\text{PF}_2)_2]_3\text{Fe}_2$ (Figure 5 and Table 3). The Fe \equiv Fe distance in the singlet $[\text{CH}_3\text{N}(\text{PF}_2)_2]_3\text{Fe}_2$ structure **IIIa** is predicted to be very

Table 3. Total Energies (E in kcal/mol), Relative Energies (ΔE in kcal/mol), Fe–Fe Distances (\AA), and Spin Expectation Values ($\langle S^2 \rangle$) for the Two Optimized $[\text{CH}_3\text{N}(\text{PF}_2)_2]_3\text{Fe}_2$ Structures

	IIIa (C_1)		IIIb (C_1)	
	B3LYP	BP86	B3LYP	BP86
$-E$	6058.60995	6059.18258	6058.61721	6059.17042
ΔE	0.0	0.0	−4.6	7.6
Fe–Fe	2.021	2.019	2.274	2.171
$\langle S^2 \rangle$	0	0	2.11	2.04
imaginary frequencies	none	none	none	none

short, namely, 2.021 \AA (B3LYP) or 2.019 \AA (BP86), corresponding to the formal quadruple bond needed to give both iron atoms the favored 18-electron configuration. In fact, **IIIa** can be regarded as derived from $\text{Fe}_2(\text{CO})_6$ by complete pairwise substitution of the six CO groups with three $\text{CH}_3\text{N}(\text{PF}_2)_2$ ligands. Although $\text{Fe}_2(\text{CO})_6$ has never been isolated or detected spectroscopically, even in low temperature matrixes, a previous DFT study⁴⁷ on a singlet unbridged structure of $\text{Fe}_2(\text{CO})_6$, using methods very similar to those used in this paper, predicts an Fe \equiv Fe distance of 2.003 \AA (B3LYP) or 2.028 \AA (BP86), which is very similar to those obtained in this work. The Fe \equiv Fe distance predicted for the triplet $[\text{CH}_3\text{N}(\text{PF}_2)_2]_3\text{Fe}_2$ structure **IIIb** of 2.274 \AA (B3LYP) or 2.171 \AA (BP86) (Figure 5 and Table 3) is significantly longer than that for the singlet structure **IIIa** and can correspond to the formal triple bond needed to give both iron atoms the 17-electron configurations for a binuclear triplet.

(47) Xie, Y.; Schaefer, H. F.; King, R. B. *J. Am. Chem. Soc.* **2000**, *131*, 8746.

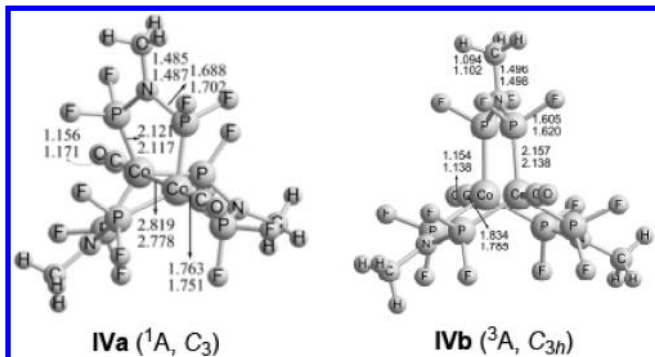


Figure 6. Two optimized $[\text{CH}_3\text{N}(\text{PF}_2)_2]_3\text{Co}_2(\text{CO})_2$ structures.

The BP86 method predicts the singlet **IIIa** to lie below the triplet by 7.6 kcal/mol, whereas the B3LYP method predicts the triplet **IIIb** to lie below the singlet by 4.6 kcal/mol. Reiher and collaborators found that B3LYP always favors the high-spin state and BP86 favors the low-spin state for a series of the Fe(II)-S complexes.⁴⁸ For this reason, they proposed a new parametrization for the B3LYP functional, named B3LYP*, which provide electronic states in agreement with experiment. In addition, these same authors tested this B3LYP* functional with the G2 test set and obtained satisfactory results.⁴⁹ For most cases the correct relative energies are between those predicted by B3LYP and BP86, possibly somewhat closer to the B3LYP values.

3.4. $[\text{CH}_3\text{N}(\text{PF}_2)_2]_3\text{Co}_2(\text{CO})_2$. Turning from iron to cobalt, two structures of $[\text{CH}_3\text{N}(\text{PF}_2)_2]_3\text{Co}_2(\text{CO})_2$ were found (Figure 6 and Table 4). The global minimum structure **IVa** is a C_3 singlet with a terminal CO group on each cobalt atom, similar to the structure determined experimentally.¹⁰ The predicted strong $\nu(\text{CO})$ frequency of 2005 cm^{-1} for **IVa** is very close to the reported¹⁰ experimental value of 2003 cm^{-1} . The predicted Co–Co distance in **IVa** of 2.819 Å (B3LYP) or 2.778 Å (BP86) is somewhat longer than the experimental Co–Co distance of 2.716 Å. However, this Co–Co distance is consistent with the single bond required to give both Co atoms the favored 18-electron configuration.

The triplet $[\text{CH}_3\text{N}(\text{PF}_2)_2]_3\text{Co}_2(\text{CO})_2$ structure **IVb** lies in energy above the singlet **IVa** by 15.7 kcal/mol (B3LYP) or 36.0 kcal/mol (BP86) (Figure 6 and Table 4). The two CO groups are terminal in **IVb**, as they are in **IVa**. The long $\text{C}_\text{O}\cdots\text{Co}$ distance in **IVb** of 3.445 Å (B3LYP) or 3.403 Å (BP86) indicates the absence of a cobalt–cobalt bond so that each cobalt atom has the 17-electron configuration required for a binuclear triplet.

3.5. $[\text{CH}_3\text{N}(\text{PF}_2)_2]_3\text{Co}_2(\text{CO})$. Four structures were optimized for the dicobalt monocarbonyl $[\text{CH}_3\text{N}(\text{PF}_2)_2]_3\text{Co}_2(\text{CO})$ (Figure 7 and Table 5). The $[\text{CH}_3\text{N}(\text{PF}_2)_2]_3\text{Co}_2(\text{CO})$ global minimum **Va** is a triplet state with C_3 symmetry and a terminal CO group on one of the cobalt atoms. The Co=Co distance in **Va** of 2.410 Å (B3LYP) or 2.349 Å (BP86) corresponds to the polarized double bond required to give each metal atom the favored 18-electron configuration. The two unpaired electrons of **Va** reside in the two orthogonal π -half-bonds of the Co=Co double

bond similar to the Fe=Fe double bond⁴⁶ in $(\eta^5\text{-C}_5\text{H}_5)_2\text{Fe}_2(\mu\text{-CO})_3$ and the double bond in triplet dioxygen.

The triplet **Va** discussed above lies significantly lower in energy than the other isomeric structures reported here. Thus a second triplet $[\text{CH}_3\text{N}(\text{PF}_2)_2]_3\text{Co}_2(\text{CO})$ structure **Vb** (Figure 7 and Table 5) has a bridging CO group and lies above **Va** by the relatively large energy of 29.6 kcal/mol (B3LYP) or 23.1 kcal/mol (BP86). Structure **Vb** has two small imaginary vibrational frequencies. However, these imaginary frequencies become real when a finer integration grid (120, 974) is used, suggesting that these imaginary frequencies arise from the numerical integration errors. The Co–Co distance in **Vb** is 2.560 Å (B3LYP) or 2.500 Å (BP86), which is $\sim 0.15\text{ Å}$ longer than the Co=Co double bond distance in the $[\text{CH}_3\text{N}(\text{PF}_2)_2]_3\text{Co}_2(\text{CO})$ structure **Va**. This is consistent with a formal single bond in **Vb**, thereby giving both Co atoms the 17-electron configurations required for a binuclear triplet.

Two relatively high energy singlet $[\text{CH}_3\text{N}(\text{PF}_2)_2]_3\text{Co}_2(\text{CO})$ structures, **Vc** and **Vd**, were found to be genuine minima (Figure 7 and Table 5). The CO group in structure **Vc** is a terminal CO group, whereas the CO group in structure **Vd** bridges the Co–Co bond. Structure **Vc** lies energetically above the global minimum **Va** by 31.1 kcal/mol (B3LYP) or 18.1 kcal/mol (BP86), while structure **Vd** lies above **Va** by 33.7 kcal/mol (B3LYP) or 16.9 kcal/mol (BP86). The Co–Co distance in **Vc** is 2.716 Å (B3LYP) or 2.672 Å (BP86) whereas that in **Vd** is significantly shorter, namely, 2.454 Å (B3LYP) or 2.444 Å (BP86). Both may be argued to be consistent with the formal single bonds required to give both cobalt atoms the favored 18-electron configuration. The shorter Co–Co distance in **Vd** relative to that in **Vc** by $\sim 0.25\text{ Å}$ may well be due to the effect of the bridging carbonyl group.

3.6. $[\text{CH}_3\text{N}(\text{PF}_2)_2]_3\text{Co}_2$. Two structures (one triplet and one singlet) were found for $[\text{CH}_3\text{N}(\text{PF}_2)_2]_3\text{Co}_2$ (Figure 8 and Table 6). The global minimum is the triplet (3A) structure **Vla**. The unpaired electron density in **Vla** is distributed approximately equally between the two cobalt atoms suggesting 17-electron configurations. This might seem to imply a formal Co=Co double bond although the Co=Co distance in **Vla** of 2.271 Å (B3LYP) or 2.217 Å (BP86) is rather short for a formal double bond.

The singlet $[\text{CH}_3\text{N}(\text{PF}_2)_2]_3\text{Co}_2$ structure **Vlb** lies above **Vla** by 32.9 kcal/mol (B3LYP) or 26.5 kcal/mol (BP86) (Figure 8 and Table 6). The Co–Co distance for **Vlb** is predicted to be 2.592 Å (B3LYP) or 2.564 Å (BP86). This can be interpreted as a formal single bond, thereby giving both cobalt atoms 16-electron configurations.

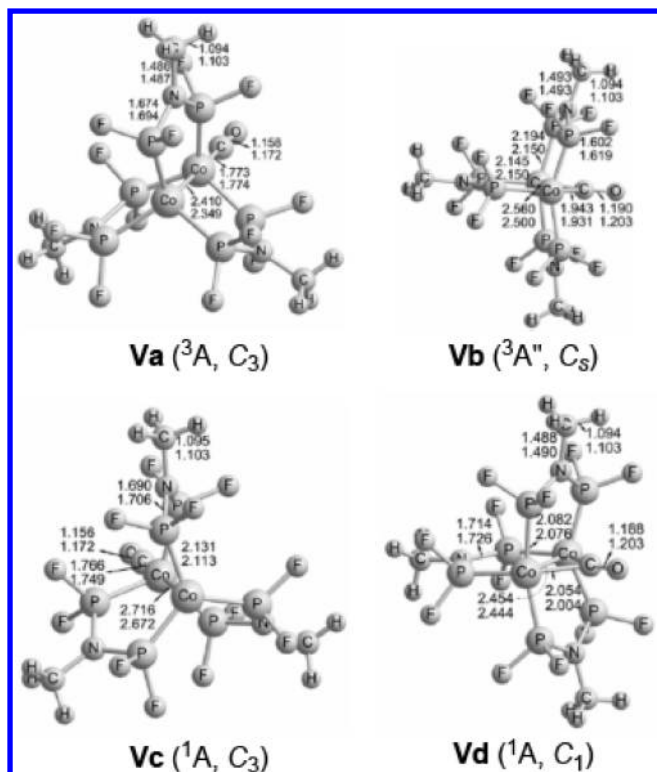
3.7. $[\text{CH}_3\text{N}(\text{PF}_2)_2]_3\text{Ni}_2(\text{CO})_2$. Two structures for the nickel compound $[\text{CH}_3\text{N}(\text{PF}_2)_2]_3\text{Ni}_2(\text{CO})_2$ were found (Figure 9 and Table 7). The C_{3h} structure **VIIa** for $[\text{CH}_3\text{N}(\text{PF}_2)_2]_3\text{Ni}_2(\text{CO})_2$ is the global minimum with a very small imaginary vibrational frequency, namely $13i\text{ cm}^{-1}$ by both the B3LYP and BP86 methods. However, this imaginary frequency is removed when the finer numerical integration grid (120, 974) is adopted. The Ni \cdots Ni distance in **VIIa** is very long, that is, 3.950 Å (B3LYP) or 3.937 Å (BP86), indicating the lack of a nickel–nickel bond. Without a nickel–nickel bond, each nickel atom in **VIIa** has the favored 18-electron configuration with an approximate tetrahedral local nickel environment analogous to $\text{Ni}(\text{CO})_4$.

(48) Reiher, M.; Salomon, O.; Hess, B. A. *Theor. Chem. Acc.* **2001**, *107*, 48.

(49) Salomon, O.; Reiher, M.; Hess, B. A. *J. Chem. Phys.* **2002**, *117*, 4729.

Table 4. Total Energies (E in kcal/mol), Relative Energies (ΔE in kcal/mol), Co–Co Distances (\AA), and Spin Expectation Values ($\langle S^2 \rangle$) for the Two Optimized $[\text{CH}_3\text{N}(\text{PF}_2)_2]_3\text{Co}_2(\text{CO})_2$ Structures

	IVa (C_3)		IVb (C_{3h})	
	B3LYP	BP86	B3LYP	BP86
$-E$	6523.56516	6524.17762	6523.54013	6524.12034
ΔE	0.0	0.0	15.7	36.0
Co–Co	2.819	2.778	3.445	3.403
$\langle S^2 \rangle$	0	0	2.05	2.01
imaginary frequencies	none	none	$6i$	$118i, 117i, 40i, 40i, 2i$

**Figure 7.** Four optimized $[\text{CH}_3\text{N}(\text{PF}_2)_2]_3\text{Co}_2(\text{CO})_2$ structures.

This singlet $[\text{CH}_3\text{N}(\text{PF}_2)_2]_3\text{Ni}_2(\text{CO})_2$ structure **VIIa** appears to be highly preferred. Thus, the lowest lying triplet $[\text{CH}_3\text{N}(\text{PF}_2)_2]_3\text{Ni}_2(\text{CO})_2$ structure **VIIb** (Figure 9 and Table 7) lies at a gigantic energy of 65.5 kcal/mol (B3LYP) or 63.4 kcal/mol (BP86) above **VIIa** and hence does not appear to be chemically significant. The Ni–Ni distance in **VIIb** is 3.108 Å (B3LYP) or 3.112 Å (BP86), which implies a rather weak interaction. However, it could correspond to a weak single bond, thereby giving each nickel atom a 19-electron configuration in this high-energy triplet structure.

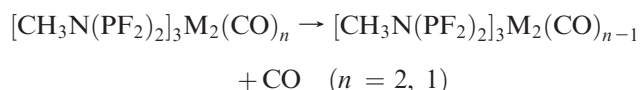
3.8. $[\text{CH}_3\text{N}(\text{PF}_2)_2]_3\text{Ni}_2(\text{CO})$. Two optimized singlet structures were found for the monocarbonyl $[\text{CH}_3\text{N}(\text{PF}_2)_2]_3\text{Ni}_2(\text{CO})$ (Figure 10 and Table 8). The singlet structure **VIIIa** with C_3 symmetry and a terminal CO group on one nickel atom is the global minimum. The Ni–Ni distance in **VIIIa** is 2.894 Å (B3LYP) or 2.656 Å (BP86). This can correspond to a single dative Ni→Ni bond from the nickel atom bearing a carbonyl group to the carbonyl free-nickel atom thereby giving both nickel atoms the favored 18-electron configuration. The higher energy but lower symmetry (C_s point group) singlet $[\text{CH}_3\text{N}(\text{PF}_2)_2]_3\text{Ni}_2(\text{CO})$ structure, namely **VIIIb**, has a

bridging CO group and lies 22.3 kcal/mol (B3LYP) or 17.1 kcal/mol (BP86) above the global minimum **VIIIa**, with a small imaginary vibrational frequency of $49i \text{ cm}^{-1}$ (B3LYP) or $58i \text{ cm}^{-1}$ (BP86). The Ni–Ni distance of 2.478 Å (B3LYP) or 2.455 Å (BP86) can correspond to the formal single bond required to give each nickel atom in **VIIIb** the favored 18-electron configuration. This Ni–Ni single bond with a carbonyl bridge supplementing the three $\text{CH}_3\text{N}(\text{PF}_2)_2$ bridges is significantly shorter than the metal–metal single bonds in $[\text{CH}_3\text{N}(\text{PF}_2)_2]_3\text{M}_2$ derivatives, without the additional carbonyl bridge such as the $[(\text{CH}_3\text{N}(\text{PF}_2)_2)_3\text{Co}_2(\text{CO})_2]$ structure **IVa** (Figure 6) at $\sim 2.8 \text{ \AA}$ (Table 5).

3.9. $[\text{CH}_3\text{N}(\text{PF}_2)_2]_3\text{Ni}_2$. Singlet and triplet $[\text{CH}_3\text{N}(\text{PF}_2)_2]_3\text{Ni}_2$ structures were found in this work (Figure 11 and Table 9). The singlet structure **IXa** is the global minimum, with beautiful C_{3h} symmetry. It has a very small imaginary frequency, namely, $1i \text{ cm}^{-1}$ (B3LYP) or $8i \text{ cm}^{-1}$ (BP86), which is removed when a finer integration grid is used. The NiP_3 units in **IXa** have 16-electron configurations in the absence of any Ni–Ni interactions. However, the Ni–Ni distance in **IXa** is 2.758 Å (B3LYP) or 2.677 Å (BP86), which is short enough to suggest some interaction between the two NiP_3 units.

A triplet structure **IXb** was also found for $[\text{CH}_3\text{N}(\text{PF}_2)_2]_3\text{Ni}_2$ at the relatively high energy of 26.9 kcal/mol (B3LYP) or 27.4 kcal/mol (BP86) above **IXa** (Figure 11 and Table 9). The Ni–Ni distance in **IXb** is 2.572 Å (B3LYP) or 2.539 Å (BP86), consistent with the formal Ni–Ni single bond needed to give both nickel atoms the 17-electron configurations for a binuclear triplet.

3.10. Dissociation Energies. Table 10 lists the bond dissociation energies (BDEs) in terms of the single carbonyl dissociation steps:



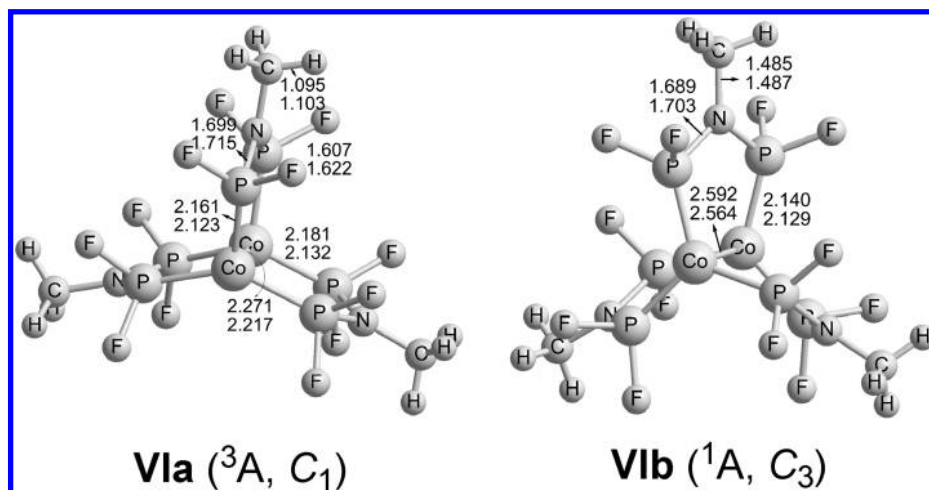
Our theoretical CO dissociation energies predicted with the BP86 method for $[\text{CH}_3\text{N}(\text{PF}_2)_2]_3\text{Fe}_2(\text{CO})_n$ (40.1 and 51.7 kcal/mol, Table 10) are comparable to the experimental dissociation energies⁵⁰ for $\text{Fe}(\text{CO})_5$ (41 kcal/mol), and those for $[\text{CH}_3\text{N}(\text{PF}_2)_2]_3\text{Ni}_2(\text{CO})_n$ (23.0 and 38.7 kcal/mol, Table 10) are comparable with the experimental dissociation energies⁵⁰ for $\text{Ni}(\text{CO})_4$ (27 kcal/mol). The theoretical CO dissociation energies for $[\text{CH}_3\text{N}(\text{PF}_2)_2]_3\text{Co}_2(\text{CO})_n$ (43.6 and 50.3 kcal/mol, Table 11) are similar to those of the iron derivatives.

(50) Sunderlin, L. S.; Wang, D.; Squires, R. R. *J. Am. Chem. Soc.* **1993**, *115*, 12060.

Table 5. Total Energies (E in kcal/mol), Relative Energies (ΔE in kcal/mol), and Co–Co Distances (Å) for the four optimized $[\text{CH}_3\text{N}(\text{PF}_2)_2]_3\text{Co}_2(\text{CO})$ Structures ^a

	Va (C_3)		Vb (C_3)		Vc (C_3)		Vd (C_1)	
	B3LYP	BP86	B3LYP	BP86	B3LYP	BP86	B3LYP	BP86
$-E$	6410.20242	6410.78094	6410.15524	6410.74421	6410.15292	6410.75217	6410.14877	6410.75408
ΔE	0.0	0.0	29.6	23.1	31.1	18.1	33.7	16.9
Co–Co	2.410	2.349	2.560	2.500	2.716	2.672	2.454	2.444
$\langle S^2 \rangle$	2.03	2.02	2.06	2.02	0	0	0	0
imaginary freqs	none	none	48i, 35i	61i, 50i	none	none	none	none

^aNote that the two imaginary vibrational frequencies for **Vb** go away with a larger integration grid.

**Figure 8.** Two optimized $[\text{CH}_3\text{N}(\text{PF}_2)_2]_3\text{Co}_2$ structures.**Table 6.** Total Energies (E in kcal/mol), Relative Energies (ΔE in kcal/mol), and Co–Co Distances (Å) for the Two Optimized $[\text{CH}_3\text{N}(\text{PF}_2)_2]_3\text{Co}_2$ Structures

	Va (C_1)		Vb (C_3)	
	B3LYP	BP86	B3LYP	BP86
$-E$	6296.79634	6297.37036	6296.74397	6269.32809
ΔE	0.0	0.0	32.9	26.5
Co–Co	2.271	2.217	2.592	2.564
$\langle S^2 \rangle$	2.18	2.05	0	0
imaginary frequencies	none	none	none	none

3.11. Vibrational Frequencies. The $\nu(\text{CO})$, $\nu(\text{CH})$, and $\nu(\text{PF})$ frequencies of the global minima were determined using the BP86 method, which has been shown to be more reliable than the B3LYP method by comparison with much available experimental data.^{51,52} These frequencies for the global minima are listed in Table 11. More comprehensive such data are provided in the Supporting Information. The $\nu(\text{PF})$ frequencies were found in the broad range of 750 to 850 cm^{-1} . The $\nu(\text{CO})$ frequencies were found in the range of 1970 to 2050 cm^{-1} , and the $\nu(\text{CH})$ frequencies were found in the broad range of 2980 to 3105 cm^{-1} .

4. Discussion

The three $\text{CH}_3\text{N}(\text{PF}_2)_2$ bridges in the $[\text{CH}_3\text{N}(\text{PF}_2)_2]_3\text{M}_2$ building blocks common to all of the structures in this paper appear to make addition of bridging carbonyls across the M–M bond of these systems energetically unfavorable, presumably because of steric hindrance. Thus, all of the

$[\text{CH}_3\text{N}(\text{PF}_2)_2]_3\text{M}_2(\text{CO})_2$ structures found in this work have exclusively terminal carbonyl groups. Furthermore, for the monocarbonyls $[\text{CH}_3\text{N}(\text{PF}_2)_2]_3\text{M}_2(\text{CO})$, unsymmetrical structures with a terminal carbonyl group on one metal atom are of lower energies than symmetrical structures in which the carbonyl group bridges the metal–metal bond.

Despite these difficulties, interpretation of the lowest energy structures of the dicarbonyls $[\text{CH}_3\text{N}(\text{PF}_2)_2]_3\text{M}(\text{CO})_2$ is straightforward in terms of the 18-electron rule. The nickel derivative $[\text{CH}_3\text{N}(\text{PF}_2)_2]_3\text{Ni}_2(\text{CO})_2$ (**VIIa** in Figure 9) has a very long $\text{Ni}\cdots\text{Ni}$ distance of ~ 3.94 Å (Table 7), indicating the absence of a direct nickel–nickel bond. The local environment of each nickel atom is a NiP_3C tetrahedron similar to that in $\text{Ni}(\text{CO})_4$. The nickel atom in **VIIa** thus has the favored 18-electron configuration.

The cobalt derivative $[\text{CH}_3\text{N}(\text{PF}_2)_2]_3\text{Co}_2(\text{CO})_2$ (**IVa** in Figure 6) is of interest since it is the one compound in this paper that has been synthesized and characterized structurally by X-ray diffraction.^{10,11} The predicted (BP86) Co–Co distance in **IVa** of 2.78 Å (Table 4) is somewhat longer than the experimental Co–Co distance of 2.72 Å. However, it is consistent with the formal Co–Co single bond required to give both cobalt atoms the favored 18-electron configuration.

The trend in the metal–metal bonding continues with the lowest energy structures of the iron compound $[\text{CH}_3\text{N}(\text{PF}_2)_2]_3\text{Fe}_2(\text{CO})_2$ (**Ia** in Figure 3). Thus its $\text{Fe}=\text{Fe}$ bond length of ~ 2.53 Å is ~ 0.2 Å shorter than that of the Co–Co bond in $[\text{CH}_3\text{N}(\text{PF}_2)_2]_3\text{Co}_2(\text{CO})_2$ and can be interpreted as the formal double bond required to give both iron atoms in $[\text{CH}_3\text{N}(\text{PF}_2)_2]_3\text{Fe}_2(\text{CO})_2$ the favored 18-electron configuration.

The lowest energy structures of the monocarbonyls $[\text{CH}_3\text{N}(\text{PF}_2)_2]_3\text{M}_2(\text{CO})$ (M = Ni, Co, Fe) have a terminal

(51) Silaghi-Dumitrescu, I.; Bitterwolf, T. E.; King, R. B. *J. Am. Chem. Soc.* **2006**, *128*, 5342.

(52) Jonas, V.; W. Thiel, W. *J. Chem. Phys.* **1995**, *102*, 8474.

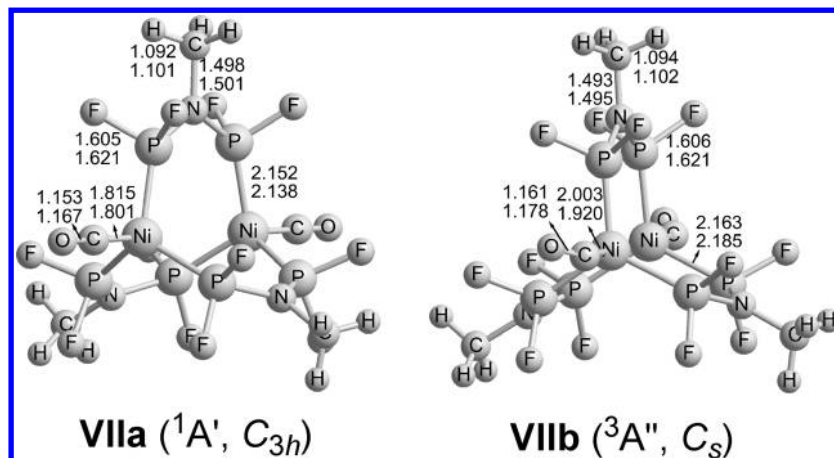


Figure 9. Two optimized [CH₃N(PF₂)₂]₃Ni₂(CO)₂ structures.

Table 7. Total Energies (E in kcal/mol), Relative Energies (ΔE in kcal/mol), and Ni–Ni Distances (Å) for the Two Optimized [CH₃N(PF₂)₂]₃Ni₂(CO)₂ Structures^a

	VIIa (C _{3h})		VIIb (C _s)	
	B3LYP	BP86	B3LYP	BP86
– E	6774.68716	6775.28993	6774.58277	6775.18888
ΔE	0.0	0.0	65.5	63.4
Ni–Ni	3.950	3.937	3.108	3.112
$\langle S^2 \rangle$	0	0	2.040	2.008
imaginary frequencies	13i	13i	205i, 19i	20i

^a Note that the imaginary frequency (13i cm^{–1}) for VIIa goes away with a larger integration grid.

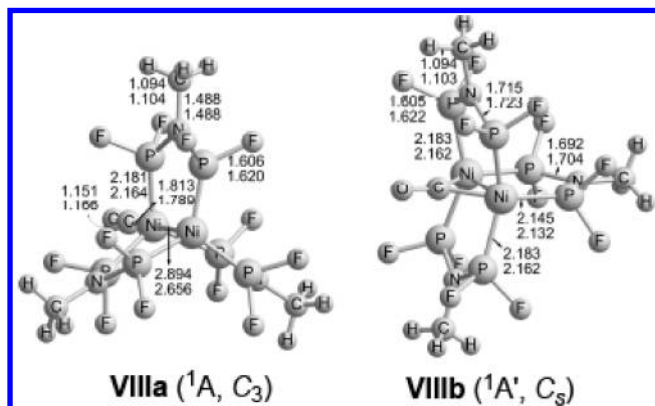


Figure 10. Two optimized [CH₃N(PF₂)₂]₃Ni₂(CO) structures.

Table 8. Total Energies (E in kcal/mol), Relative Energies (ΔE in kcal/mol), and Ni–Ni Distances (Å) for the Two Optimized [CH₃N(PF₂)₂]₃Ni₂(CO) Structures

	VIIIa (C ₃)		VIIIb (C _s)	
	B3LYP	BP86	B3LYP	BP86
– E	6661.32543	6661.92601	6661.28984	6661.89875
ΔE	0.0	0.0	22.3	17.1
Ni–Ni	2.894	2.656	2.478	2.455
imaginary frequencies	none	none	49i	58i

carbonyl group rather than a bridging carbonyl group so that the two metal atoms are non-equivalent. Because of this asymmetry a metal→metal dative bond of some type is required to equalize the electronic configuration of the

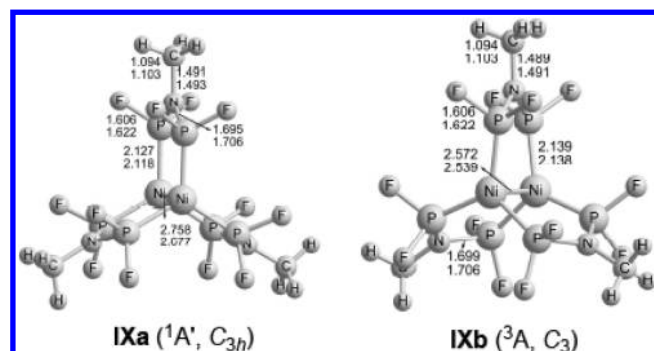


Figure 11. Two optimized [CH₃N(PF₂)₂]₃Ni₂ structures.

Table 9. Total Energies (E in kcal/mol), Relative Energies (ΔE in kcal/mol), and Ni–Ni Distances (Å) for the Two Optimized [CH₃N(PF₂)₂]₃Ni₂ Structures^a

	IXa (C _{3h})		IXb (C ₃)	
	B3LYP	BP86	B3LYP	BP86
– E	6547.95089	6548.53711	6547.90806	6548.49350
ΔE	0.0	0.0	26.9	27.4
Ni–Ni	2.758	2.677	2.572	2.539
$\langle S^2 \rangle$			2.02	2.00
imaginary frequencies	1i	8i	none	8i

^a For IXa the larger integration grid removes the very small imaginary vibrational frequency.

two metal atoms (Figure 12). For [CH₃N(PF₂)₂]₃Ni₂(CO) (VIIIa in Figure 10) the Ni→Ni distance of ~2.77 Å (average of B3LYP and BP86 results) can be interpreted as a dative single bond from the nickel bearing the carbonyl group to the carbonyl-free nickel atom so that each nickel atom has the favored 18-electron configuration.

The lowest energy structure of [CH₃N(PF₂)₂]₃Co₂(CO) (Va in Figure 7) is a triplet rather than a singlet. Its much shorter Co=Co distance of ~2.38 Å can be interpreted as a formal double bond, thereby giving each cobalt atom the favored 18-electron configuration. The triplet spin multiplicity in Va arises from the Co=Co double bond being of the $\sigma + ^2/2\pi$ type with the two unpaired electrons being the single electrons in the two π “half-bonds”. Similar formal double bonds are found not only in dioxygen but also in the binuclear iron derivative (η^5 -C₅H₅)₂Fe₂(μ -CO)₃.⁴⁶

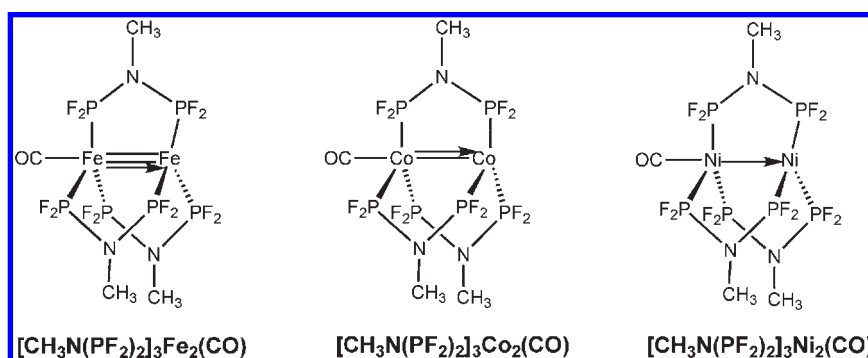
Table 10. Energies (in kcal/mol) for Carbonyl Dissociation Reactions

	ΔE	
	B3LYP	BP86
$[\text{CH}_3\text{N}(\text{PF}_2)_2]_3\text{Fe}_2(\text{CO})_2$ (Ia) \rightarrow $[\text{CH}_3\text{N}(\text{PF}_2)_2]_3\text{Fe}_2(\text{CO})$ (IIa)+CO	29.6	40.1
$[\text{CH}_3\text{N}(\text{PF}_2)_2]_3\text{Fe}_2(\text{CO})$ (IIa) \rightarrow $[\text{CH}_3\text{N}(\text{PF}_2)_2]_3\text{Fe}_2$ (IIIa)+CO	44.3	51.7
$[\text{CH}_3\text{N}(\text{PF}_2)_2]_3\text{Co}_2(\text{CO})_2$ (IVa) \rightarrow $[\text{CH}_3\text{N}(\text{PF}_2)_2]_3\text{Co}_2(\text{CO})$ (Va)+CO	21.4	43.6
$[\text{CH}_3\text{N}(\text{PF}_2)_2]_3\text{Co}_2(\text{CO})$ (Va) \rightarrow $[\text{CH}_3\text{N}(\text{PF}_2)_2]_3\text{Co}_2$ (VIa)+CO	48.6	50.3
$[\text{CH}_3\text{N}(\text{PF}_2)_2]_3\text{Ni}_2(\text{CO})_2$ (VIIa) \rightarrow $[\text{CH}_3\text{N}(\text{PF}_2)_2]_3\text{Ni}_2(\text{CO})$ (VIIIa)+CO	20.8	23.0
$[\text{CH}_3\text{N}(\text{PF}_2)_2]_3\text{Ni}_2(\text{CO})$ (VIIIa) \rightarrow $[\text{CH}_3\text{N}(\text{PF}_2)_2]_3\text{Ni}_2$ (IXa)+CO	28.8	38.7

Table 11. Theoretical Vibrational Frequencies (in cm^{-1}) $\nu(\text{PF})$, $\nu(\text{CO})$, and $\nu(\text{CH})$ for All Global Minima Predicted by the BP86 Method^a

	$\nu(\text{P}-\text{F})$	$\nu(\text{C}-\text{O})$	$\nu(\text{C}-\text{H})$
Ia	767(19), 767(64), 768(15), 778(298), 781(7), 783(66), 786(10), 789(108), 800(87), 805(724), 807(682), 838(9)	1971(1756), 1981(85)	2996(65), 2996(6), 2997(25), 3083(7), 3084(5), 3084(9), 3093(3), 3093(3), 3097(2)
IIa	763(128), 767(20), 774(24), 776(22), 779(180), 781(81), 789(87), 790(66), 794(187), 809(544), 813(626), 832(194)	1980(896)	2990(43), 2992(35), 2994(32), 3077(8), 3078(8), 3080(8), 3085(3), 3090(3), 3091(3)
IIIa	753(126), 758(9), 760(12), 772(24), 776(29), 777(104), 779(77), 781(83), 787(426), 804(629), 806(810), 830(155)		2987(46), 2994(40), 2994(32), 3073(9), 3081(7), 3081(9), 3085(3), 3089(3), 3092(2)
IVa	769(3), 769(3), 773(24), 773(24), 774(59), 776(0), 786(348), 787(49), 787(49), 798(764), 798(764), 835(0)	2005(1338), 2010(0)	2996(52), 2996(52), 2997(1), 3083(1), 3083(11), 3083(11), 3096(0), 3096(0), 3096(6)
Va	767(72), 767(72), 768(5), 779(96), 779(96), 780(16), 784(102), 784(102), 785(387), 805(574), 805(574), 835(4)	2003(863)	2995(50), 2995(50), 2995(0), 3084(0), 3085(10), 3085(10), 3089(0), 3089(0), 3089(8)
VIa	754(79), 760(25), 765(13), 769(17), 772(77), 776(143), 778(17), 782(148), 783(370), 797(736), 801(749), 835(22)		2993(52), 2993(28), 2996(35), 3080(7), 3081(8), 3083(8), 3088(3), 3091(2), 3094(3)
VIIa	768(0), 773(0), 773(0), 775(0), 782(0), 782(0), 784(127), 784(127), 796(715), 796(715), 801(299), 823(0)	2024(1453), 2028(0)	3008(44), 3008(44), 3008(0), 3101(0), 3101(8), 3101(8), 3105(2), 3105(0), 3105(0)
VIIIa	769(57), 769(57), 774(7), 774(7), 774(11), 775(93), 785(106), 785(106), 787(229), 799(630), 799(630), 842(106), 842(106)	2037(724)	2995(57), 2995(57), 2995(0), 3082(1), 3082(11), 3082(11), 3097(1), 3097(1), 3097(7)
IXa	763(1), 766(0), 766(0), 771(0), 778(0), 778(0), 780(50), 780(50), 796(869), 796(869), 803(605), 842(0)		3000(53), 3000(53), 3000(0), 3090(0), 3090(11), 3090(11), 3095(0), 3095(0), 3095(5)

^a The infrared intensities are given in parentheses in km/mol .

**Figure 12.** Schematic representation of the metal–metal dative bonds in the monocarbonyls $[\text{CH}_3\text{N}(\text{PF}_2)_2]_3\text{M}_2(\text{CO})$ ($\text{M} = \text{Fe}, \text{Co}, \text{Ni}$).

The lowest energy structure of $[\text{CH}_3\text{N}(\text{PF}_2)_2]_3\text{Fe}_2(\text{CO})$ (**IIa** in Figure 4) is a singlet like that of $[\text{CH}_3\text{N}(\text{PF}_2)_2]_3\text{Ni}_2(\text{CO})$ (**VIIIa** in Figure 10). The $\text{Fe}\equiv\text{Fe}$ distance of ~ 2.13 Å is ~ 0.25 Å shorter than the $\text{Co}=\text{Co}$ distance in **Va** and thus can be interpreted as the formal iron–iron triple bond needed to give both iron atoms in **IIa** the favored 18-electron configuration. In this case, one of the components of this $\text{Fe}\equiv\text{Fe}$ triple bond is a dative bond, from the iron bearing the carbonyl group to the carbonyl-free iron (Figure 12).

The metal–metal bonding in the carbonyl-free derivatives $[\text{CH}_3\text{N}(\text{PF}_2)_2]_3\text{M}_2$ ($\text{M} = \text{Fe}, \text{Co}, \text{Ni}$) can be interpreted analogously after consideration of the following two points:

- (1) The structures are symmetrical so that the metal–metal bonds have no dative components;
- (2) The absence of strongly π -back bonding carbonyl groups increases the electron density on the

metal atoms, so that the metal–metal bond distances are shorter for a given bond order.

In connection with these two points, the lowest energy structure for $[\text{CH}_3\text{N}(\text{PF}_2)_2]_3\text{Ni}_2$ (**IXa** in Figure 11) is a singlet with a $\text{Ni}=\text{Ni}$ distance of ~ 2.72 Å. Although this distance is approximately equal to the $\text{Co}-\text{Co}$ single bond distance in $[\text{CH}_3\text{N}(\text{PF}_2)_2]_3\text{Co}_2(\text{CO})_2$ (**IVa** in Figure 6), the $\text{Ni}=\text{Ni}$ interaction is best interpreted as the formal double bond needed to give both nickel atoms the favored 18-electron configuration. For $[\text{CH}_3\text{N}(\text{PF}_2)_2]_3\text{Co}_2$ (**VIa** in Figure 8) the lowest energy structure is a triplet with a relatively short $\text{Co}=\text{Co}$ distance of ~ 2.24 Å. This distance would suggest a formal triple bond. However, a formal double bond is what is needed to give the cobalt atoms the 17-electron configurations for a binuclear triplet. The lowest energy structure of $[\text{CH}_3\text{N}(\text{PF}_2)_2]_3\text{Fe}_2$ (**IIIa** in Figure 5), like that of the analogous nickel derivative, is a

singlet state with the shortest metal–metal distance of any of the structures encountered in this work, namely, ~ 2.02 Å. This short Fe \equiv Fe bond is thus readily interpreted as the formal quadruple bond required to give both iron atoms the favored 18-electron configuration. This finding is important, since no iron–iron quadruple bond is yet known from experiment.

Acknowledgment. We are indebted to the 111 Project (B07012) and the National Natural Science Foundation (20873045) of China as well as the U.S. National Science

Foundation (Grants CHE-0749868 and CHE-0716718) for support of this research.

Supporting Information Available: Tables S1 to S21, harmonic vibrational frequencies for the $[\text{CH}_3\text{N}(\text{PF}_2)_2]_3\text{M}_2(\text{CO})_n$ ($\text{M} = \text{Fe}, \text{Co}, \text{Ni}; n = 2, 1, 0$) structures; Tables S22 to S42, atomic coordinates for the optimized $[\text{CH}_3\text{N}(\text{PF}_2)_2]_3\text{M}_2(\text{CO})_n$ ($\text{M} = \text{Fe}, \text{Co}, \text{Ni}; n = 2, 1, 0$) structures; complete Gaussian 03 reference (Reference 40). This material is available free of charge via the Internet at <http://pubs.acs.org>.